The influence of tertiary butyl hydrazine as a co-reactant on the atomic layer deposition of silver

Applied Surface Science 399 (2017) 123–131

Contents lists available at ScienceDirect

Applied Surface Science

journal homepage: www.elsevier.com/locate/apsusc

Full Length Article

The influence of tertiary butyl hydrazine as a co-reactant on the atomic layer deposition of silver

Zahra Golrokhi[a], Paul A. Marshall[a], Simon Romani[a], Simon Rushworth[b], Paul R. Chalker[a], Richard J. Potter[a,*]

[a] Centre for Materials and Structures, School of Engineering,The University of Liverpool, Liverpool L69 3GH, UK
[b] EpiValence, The Wilton Centre, Redcar, Cleveland, TS10 4RF, UK

ARTICLE INFO

Article history:
Received 23 September 2016
Received in revised form
22 November 2016
Accepted 24 November 2016
Available online 11 December 2016

Keywords:
Atomic layer deposition
Self limiting
Silver thin films
Tertiary butyl hydrazine

ABSTRACT

Ultra-thin conformal silver films are the focus of development for applications such as anti-microbial surfaces, optical components and electronic devices. In this study, metallic silver films have been deposited using direct liquid injection thermal atomic layer deposition (ALD) using (hfac)Ag(1,5-COD) ((hexafluoroacetylacetonato)silver(I)(1,5-cyclooctadiene)) as the metal source and tertiary butyl hydrazine (TBH) as a co-reactant. The process provides a 23 °C wide 'self-limiting' ALD temperature window between 105 and 128 °C, which is significantly wider than is achievable using alcohol as a co-reactant. A mass deposition rate of ~20 ng/cm^2/cycle (~0.18 Å/cycle) is observed under self-limiting growth conditions. The resulting films are crystalline metallic silver with a near planar film-like morphology which are electrically conductive. By extending the temperature range of the ALD window by the use of TBH as a co-reactant, it is envisaged that the process will be exploitable in a range of new low temperature applications.

1. Introduction

Thermal atomic layer deposition (ALD) offers a highly desirable and perhaps even 'unique' combination of attributes that makes it highly attractive as a manufacturing process for applications where ultra-thin, conformal, pinhole-free coatings are required. Many of the desirable characteristics of ALD are directly related to the saturative surface reactions that are at the heart of 'self-limiting' ALD processes. The key advantages of ALD are, however, only realisable within a limited window of process parameters (temperatures, pressures, dose times, purge times etc) for each particular set of chemical reactants. In thermal ALD, temperature is a fundamentally important process parameter and the term 'ALD window' is widely used to define the range over which growth rate is independent of temperature. In terms of manufacturing, a wide 'ALD window' is advantageous as it means that larger spatial or temporal fluctuations in temperature can be tolerated, thus making the process intrinsically more stable, repeatable and easier to control. A reasonably wide ALD window is particularly important for coating large or complex three dimensional objects as uniform heating can be challenging.

The controlled deposition of ultra-thin conformal silver films is of great interest for applications such as anti-microbial surfaces [1], plasmonic enhanced thin film photovoltaics [2], highly reflective mirrors, catalysts [3] and gas sensors [4]. Relatively few studies on the ALD of metallic silver have been reported. Several have exploited plasma enhanced (PE) or radical enhanced (RE) ALD [5–8] and fewer have addressed thermal ALD [9–11] which is intrinsically more scaleable over larger areas. The plasma or radical enhanced ALD approach uses highly reactive co-reactant species which are generated from a plasma source, which offers both advantages and challenges in comparison to thermal ALD [12].

.One major advantage of PEALD (or REALD) is the use highly reactive species that are able to drive forward the surface reactions even at low temperatures, which means that they tend to extend the low temperature end of the ALD process window. For PEALD or REALD of silver, ALD windows of 20 °C has been reported [6], which is significantly wider than reported to-date for thermal ALD, where just one study has confirmed a 5 °C window [11]. On the flip side, one challenge associated with PEALD or REALD processes is that they rely on short-lived co-reactant species. The limited lifetime of these reactive species can become an issue if the process is to be used

* Corresponding author.
E-mail address: rjpott@liverpool.ac.uk (R.J. Potter).

http://dx.doi.org/10.1016/j.apsusc.2016.11.192

to coat very large substrate areas or complex three-dimensional structures, particularly high aspect ratio ones.

The thermal ALD of ultrathin silver films has built on the earlier chemical vapour deposition (CVD) research, which has tended to focus on organofluoro complexes, amongst others. For example, Bahlawane et al. [13], demonstrated the growth of silver films by CVD using (hfac)Ag(1,5-COD) ((hexafluoroacetylacetonato)silver(I)(1,5-cyclooctadiene)) and various alcohols. The process exploits the catalytic reactivity of cationic silver, and the reactivity of alcohols with silver surfaces, whereby the affinity of cationic silver to alcohols and aldehydes leads to its chemical reduction. The same precursor has also been used to grow silver films in supercritical CO_2 using H_2 and acetone as the reducing agents [14]. However, the cyclic dosing of the precursor and co-reagent used in the ALD approach allows the influence of surface chemistry to dominate the growth mechanism. Liquid injection ALD was first used to demonstrate the growth of silver nanoparticles (NPs) [10] using the organometallic precursor (hfac)Ag(1,5-COD) dissolved in a 0.1 M toluene solution. The silver adsorbate species was reduced to metallic Ag NPs using intermittent pulses of propan-1-ol. Transmission electron microscopy reveals that the NPs deposited in the temperature range 110 °C–250 °C consist of face centred cubic, facetted silver crystallites. We have recently extended this work to establish the self-limiting growth regime for this process, hence enabling the deposition of ultra-thin conformal polycrystalline silver films [11]. Self-limiting growth was achieved within a narrow ALD temperature window between 123 and 128 °C which showed a mass deposition rate of ~17.5 ng per cm^2 per cycle. Pure metallic silver film with subsequent adsorption of atmospheric contaminants from air exposure was achieved in that study. The potential for exploiting other co-reactants for thermal ALD of silver, such as substituted hydrazine's (R_1HNNHR_2 where R_1 and R_2 represent alkyl substitution for example) was recognised by our group some time ago, leading to work that helped to support a patent application for SAFC Hitech [15].

The use of hydrazine based co-reactants in thermal ALD has not been widely reported to-date. A few studies report on the use of hydrazine based co-reactants as nitrogen sources for the deposition of metal nitrides [16–18]. To the best of our knowledge, only one experimental study by Knisley et al. [19] has previously reported on the use of hydrazine as a co-reactant for the ALD of a metal. Metallic copper was deposited using a three stage ALD process involving $Cu(dmap)_2$ (dmap = $OCHMeCH_2$–NMe_2), formic acid and un-substituted hydrazine. The formic acid is believed to form a copper formate, which is subsequently reduced to copper metal by the un-substituted hydrazine. The reaction scheme has been further elucidated by Dey and Elliot [20] via Density Functional Theory (DFT) modelling. The DFT study indicated that the formation of a formate intermediary is energetically viable during the first co-reactant dosing steps. The DFT study suggest that the hydrazine partially oxidises the formate, which then decomposes to CO_2 and in doing so reduces $Cu^{(+1)}$ to $Cu^{(0)}$. This DFT study indicates that co-reagents for metal ALD may not need to be limited to traditional reducing agents, but could also include reagent combinations that release electrons during oxidative decomposition [20]. Irrespective of the actual reaction mechanism in the Knisley study [19], they show that the un-substituted hydrazine on its own is not sufficient to form metallic copper from the $Cu(dmap)_2$ within the ALD temperature window.

In the current study, we looked at using a substituted hydrazine for the ALD of metallic silver. The choice of hydrazine derivative was based upon reaction chemistry to provide a single pathway to the target film while avoiding incorporation of unwanted elements. Un-substituted hydrazine (H_2NNH_2) in its anhydrous state is a toxic hazardous material that has explosive tendencies and so substitution to reduce risk is necessary for any process that is desired to be scaled safely to production volumes. The symmetric and unsymmetric dimethylhydrazines (MeHNNHMe, Me_2NNH_2) have been widely employed as alternatives however in the ALD process where surface reactions control the layer growth both compounds lead to the delivery of –Me groups to the surface that could lead to deleterious incorporation of carbon. To reduce the risk of such inclusions the tButyl substituted hydrazine ($tBuHNNH_2$) was chosen due to the beta hydride elimination pathway available to remove the tButyl group in a facile manner reducing potential C contamination [21]. In effect this enables the formation of H_2NNH_2 in situ at the surface which is sufficiently reactive to deposit metallic silver films.

Table 1
ALD growth conditions.

Growth condition	Value			
Growth temperature	80–200 °C			
Reactor pressure	5 mbar			
Silver precursor	(hfac)(1,5-COD)Ag			
Silver source	0.1 M solution in n-Toluene			
Vaporizer temperature	130 °C			
Precursor delivery rate	17.5 μl/s			
Argon flow rate	200 sccm			
Co-reactant	Tertiary butyl hydrazine			
Co-reactant delivery	Vapour draw at ~20 °C			
ALD cycle	Inject	Purge	TBH	Purge
	0–6 s	4 s	0–4 s	0.5 or 4 s

The pKa value for TBH is 8.1 [22] whereas; the pKa for both propan-1-ol and butan-1-ol is 16.1 [23]. Therefore, alcohols are less acidic compared with hydrazines and so less favourable proton donors [24]. In this paper, a self-limiting thermal ALD process for the deposition of metallic silver thin films using TBH is presented and compared with the alcohol based silver ALD process previously presented [10,11]. To the best of our knowledge, this is the first ALD study that uses a substituted hydrazine as a co-reactant for the deposition of a metal. In this paper, we investigate the effect of using TBH as a reactive co-reagent for the thermal ALD of silver films. The purpose of this is to extend the "surface limiting" ALD process to lower temperatures and to examine the effect of this on the morphology of the silver films.

2. Experimental procedure

2.1. ALD growth experiments

Films were deposited on as-supplied polished virgin test grade Si(100) (Compart Technology Ltd) and on soda-lime glass slides (Fisher Scientific) using a customised Aixtron AIX 200FE^{TM} reactor as described in reference [25]. A 0.1 M solution of (hfac)Ag(1,5-COD) (SAFC Hitech) in anhydrous toluene (Sigma Aldrich) was used as the silver source. This solution was introduced into the reactor by direct liquid injection via a Jipelec^{TM} vaporiser with a set-point temperature of 130 °C. The growth method and equipment used here replicates that used in our previous reported silver ALD study [11] except that the propan-1-ol was replaced with tertiary butyl hydrazine (TBH) (98%, HPLC grade supplied by SAFC Hitech Ltd) as the co-reactant. The TBH was introduced into the reactor via a Swagelok ALD valve using conventional vapour-draw sources held at room temperature (~20 °C). Further details of the growth conditions are described in reference [11] and are summarised in Table 1.

2.2. Physico-chemical characterisation

Film deposition rate was evaluated gravimetrically by measuring the mass change of 40 × 40 mm Si(100) samples after deposition

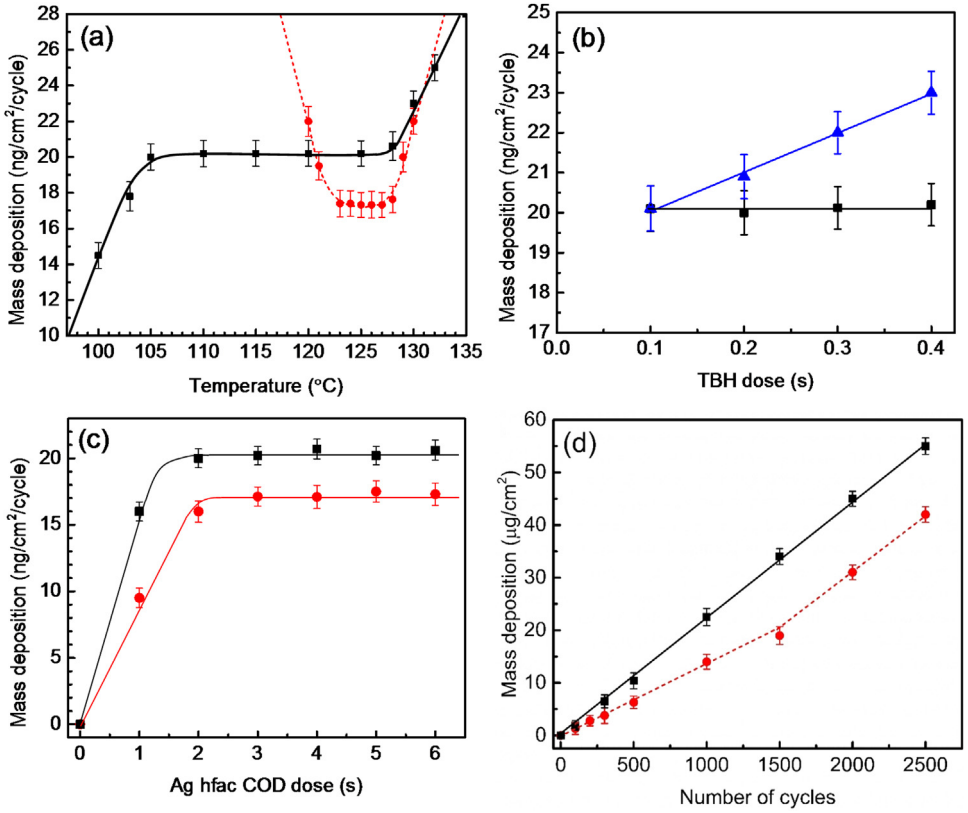

Fig. 1. (a) Mass deposition rate as a function of substrate temperature using 4 s doses of (hfac)Ag(1,5-COD) and 4 s purges with either 0.2 s TBH doses as a co-reactant (black squares) or with 4 s propan-1-ol doses as a co-reactant (red circles); (b) Mass deposition rate as a function of TBH dose at 2 different purge times, at 115 °C with 4 s (hfac)Ag(1,5-COD) doses and either 0.5 s (blue triangle) or 2 s (black squares) purges; (c) Mass deposition rate as a function of (hfac)Ag(1,5-COD)dose with either TBH at 115 °C (black squares) or with propan-1-ol at 125 °C (red circles) for 500 ALD cycles; (d) Total mass deposition per unit area as a function of number of ALD cycles for TBH at 115 °C (black squares) and with Propan-1-ol at 125 °C (red circles). (For interpretation of the references to colour in this figure legend, the reader is referred to the web version of this article.)

using a Mettler Toledo XS205-DU™ analytical micro balance. As a first approximation, nominal film thickness was estimated by assuming a bulk silver density of 10.5 g/cm^3. Film microstructure and topography was analysed using X-ray diffraction (XRD), scanning electron microscopy (SEM) and high resolution transmission electron microscopy (HRTEM) while the chemical composition was investigated using X-ray photoelectron spectroscopy (XPS). XRD was carried out on films deposited on Si(100) using a Bragg-Brentano diffractometer (Rigaku-miniflex™) with a Cu Kα1 source (λ = 1.5405 Å). SEM was carried out using a JEOL JSM-7001F™ FEG-SEM for films grown on Si(100). HRTEM imaging was performed using a JEOL 2100F FEGTEM at 200 kV to acquire detailed micrographs of Ag films deposited onto supported 50 nm thick SiN membranes (Agar Scientific). SiN TEM support membranes offer a convenient way of carrying out TEM imaging of ultra-thin coatings without the need for extensive sample processing, which could damage the microstructure being studied. XPS measurements were carried out using a FISONS VG Escalab MKII with an Al Kα x-ray source (1486.6 eV). A custom built four point probe (4PP) system based on a Signatone probe head (SP4-50085TFS™) and a Keithley 2400 source meter were used to assess the resistivity of silver films deposited onto soda-lime glass. The adhesion of the films to Si(100) was evaluated semi-quantitatively using the 'Scotch tape test' and SEM. SEM image analysis was carried out using the macro particle size analyser (PSA r12) plugin in ImageJ [26] sampling 1 μm^2 areas. Each sample was analysed by randomly sampling at least four areas to ensure that the resulting data was representative of the whole. The adhesion tests used SEM image analysis to compare the pre-test surface coverage with the surface after the application and removal of Scotch® 600 transparent tape.

3. Results and discussions

3.1. Film growth study

The effects of deposition temperature on the ALD growth rate using TBH as a co-reactant was investigated between 80 °C and 200 °C. The mass gain per cycle was evaluated after 500 ALD cycles, using 4 s doses of (hfac)Ag(1,5-COD), 0.2 s TBH doses and 4 s purges. The results (between 95 and 135 °C) are shown in Fig. 1(a) along with data for the propan-1-ol based process [11] for comparison. For the TBH process, a plateau region is observed between 105 and 128 °C and within this range the average mass deposition rate is ~20 ng/cm^2/cycle. This 23 °C wide plateau region defines an ALD window with a nominal growth rate of ~0.18 Å/cycle. Using TBH as a co-reactant results in a significant enhancement in the width of the ALD temperature window compared to that obtained using propan-1-ol [11] where the plateau region is just 5 °C wide. The TBH also appears to enhance the ALD growth rate by ~3 ng/cm^2/cycle compared to propan-1-ol. The ALD window width obtained using TBH is similar to that reported for PEALD of silver [6].

As with the propan-1-ol based process, the mass deposition rate increases rapidly as the temperature increases above 128 °C and this is attributed to thermal decomposition of the silver precursor, which results in a CVD-like contribution to the mass gain. As the temperature decreases below 105 °C, the mass deposition rate drops; at these temperatures there is likely to be insufficient thermal energy to drive the surface reactions to completion.

To confirm that the ALD deposition process with TBH is controlled by self-limiting surface reactions and to establish suitable processing conditions, the effects of co-reactant dose, purge, pre-

cursor dose and ALD cycles were investigated at 115 °C (the middle of the ALD temperature window). To investigate the effect of TBH dose and purge times, films were grown using 500 ALD cycles with 4 s doses of the silver precursor and either 0.5 or 2 s purges (Fig. 1(b)). To confirm that the co-reactant is responsible for the measured mass gain, runs were also carried out without TBH doses and no mass gain was detected. With 0.5 s purges, the mass deposition rate increases from ~20 to ~23 ng/cm^2/cycle as the TBH dose increases from 0.1 to 0.4 s. However, with 2 s purges, the mass deposition rate remains constant at ~20 ng/cm^2 per cycle (Fig. 1b). The constant mass deposition rate with TBH dose using 2 s purges is consistent with a process controlled by saturative surface reactions. The increase in mass deposition rate observed using 0.5 s purges is attributed to gas-phase mixing of the two reactants due to insufficient purges times. This mixing leads to gas phase reactions between the reactants, which causes a CVD-like contribution to the growth.

To investigate the effect of (hfac)Ag(1,5-COD) dose on the deposition rate, films were grown using 500 ALD cycles with 0.2 s doses TBH and 4 s purges. The mass deposition rate initially increases with the precursor dose, but saturates at ~20 ng/cm^2/cycle for doses above ~2 s as shown in Fig. 1(c). This saturation behaviour of the silver precursor with TBH as a co-reactant is in good agreement with the results of the propan-1-ol process [11] at 125 °C (the middle of the narrow ALD window for the propan-1-ol process) also shown in Fig. 1(c), indicating the both processes are controlled by self-limiting surface reactions.

The effect of ALD cycle number on the overall mass deposition was studied to further explore the nucleation and growth process. For this experiment, films were deposited at 115 °C using 4 s doses of the silver precursor, 0.2 s TBH doses (or 4 s propan-1-ol doses) and 4 s purges; parameters selected to be well within the saturative dosing and necessary purging regime for self-limiting ALD. The results of this study are shown in Fig. 1(d). As expected from a 'well behaved' ALD process, the total mass deposition for the TBH based ALD process is directly proportional to the number of cycles. The slope of the line is around 20 ng/cm^2/cycle, which corresponds to a nominal growth rate of ~0.18 Å/cycle. The results for the comparative propan-1-ol based process (at 125 °C) are somewhat more complex. The overall mass gain appears to increase linearly with ALD cycles up to around 1500 cycles, and then the slope increases. The initial slope (~17 ng/cm^2/cycle) is significantly lower than for the TBH based process, which is attributed to the way in which silver nucleates and grows as 3D islands when using the propan-1-ol based ALD process [11]. However, as the number of cycles exceeds ~1500, the slope of the line becomes almost identical to the TBH line. As the propan-1-ol process is driven by a catalytic process mediated by the silver on the surface [13], it is likely that the initial growth rate is influenced by the limited surface coverage of silver.

3.2. Composition analysis

In order to study the chemical composition of the silver films, selected samples were analysed using XPS. Fig. 2(a) shows a survey scan (200–750 eV) of films deposited on Si(100) at 115 °C using 500 cycles with 4 s of silver precursor doses, 0.2 s of TBH doses (or 4 s propan-1-ol doses) and 4 s purges. Features relating to silver, carbon and oxygen are visible on both spectra, while the fluorine feature at 688.87 eV is only detected in the sample grown using propan-1-ol as a co-reactant. The presence of the F1s features in the XPS is attributed to incomplete removal of the hfac ligands or at least fragments of it from the surface. As previously reported for the propon-1-ol based ALD process [11], the F1s XPS feature is only visible in films grown at temperature below the ALD-window minima. To further investigate the incorporation of fluorine, detailed XPS scans were taken for films grown using TBH at temperatures ranging from 80 to 135 °C (Fig. 2(b)). No visible F1s peaks are observed at growth temperatures above 105 °C (the minima of the ALD window) indicating that the fluorine is below the detection limit of the XPS system (~1 at.%). At temperatures below 105 °C the F1s peak intensity increases almost linearly with decreasing temperature. As the mass deposition rate (Fig. 1a) for the TBH process decreases at these low growth temperatures, condensation of the silver source seems unlikely and hence the fluorine incorporation is attributed to reaction rates. At these low temperatures, there is insufficient thermal energy to fully reduce the silver precursor on the surface and hence the mass deposition rate decreases as some un-reacted precursor is left on the surface at the end of each cycle. The un-reacted precursor left on the surface at the end of one cycle may well react with the co-reactant during the subsequent cycle. The absence of the F1s feature at temperatures between 105 and 128 °C gives a good initial indication that the ALD surface reaction are 'clean' within the ALD window.

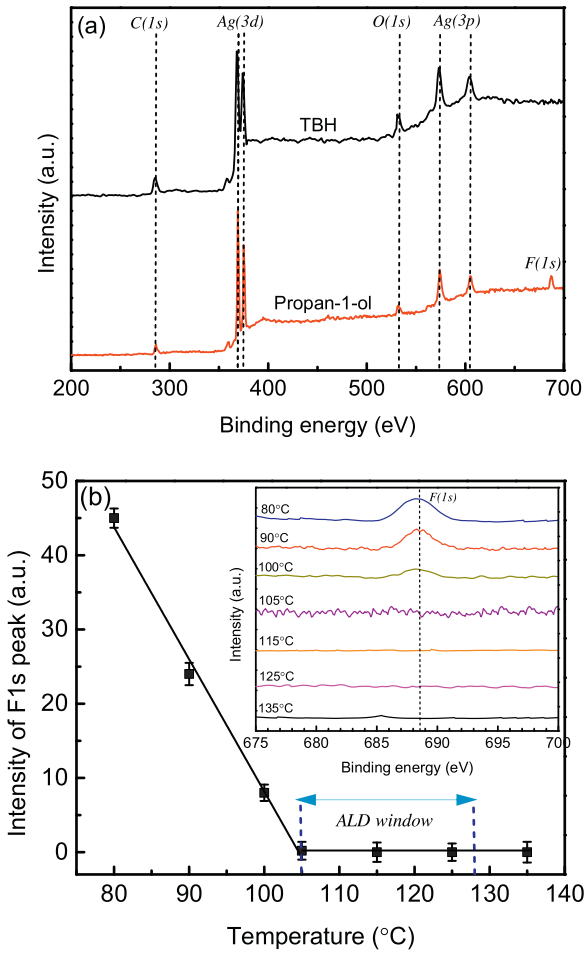

Fig. 2. (a) XPS survey scan of Ag films deposited by ALD on Si(100) at 115 °C with either 0.2 s of TBH doses or4 s of propan-1-ol doses; (b) Variation in XPS peak intensities of F1 s at different temperatures with TBH dose.

As it was not possible to carry out in-situ surface cleaning of samples within our XPS system, signals from atmospheric absorbates on the surface are expected to be observed. To establish the origin of the carbon and oxygen XPS features, high resolution XPS of the C1s (not shown), O1s (Fig. 3a and b) and Ag3d (Fig. 3c and d) features were obtained for films grown at 80 and 115 °C. The C1s peaks are centred at 284.8 eV, which corresponds to C—C or C—H bonding states and is attributed to surface absorbates rather than bulk incorporation [27]. The O1s feature for the film grown at 115 °C (Fig. 3a) is readily fitted with a single Gaussian centred at 532.4 eV,

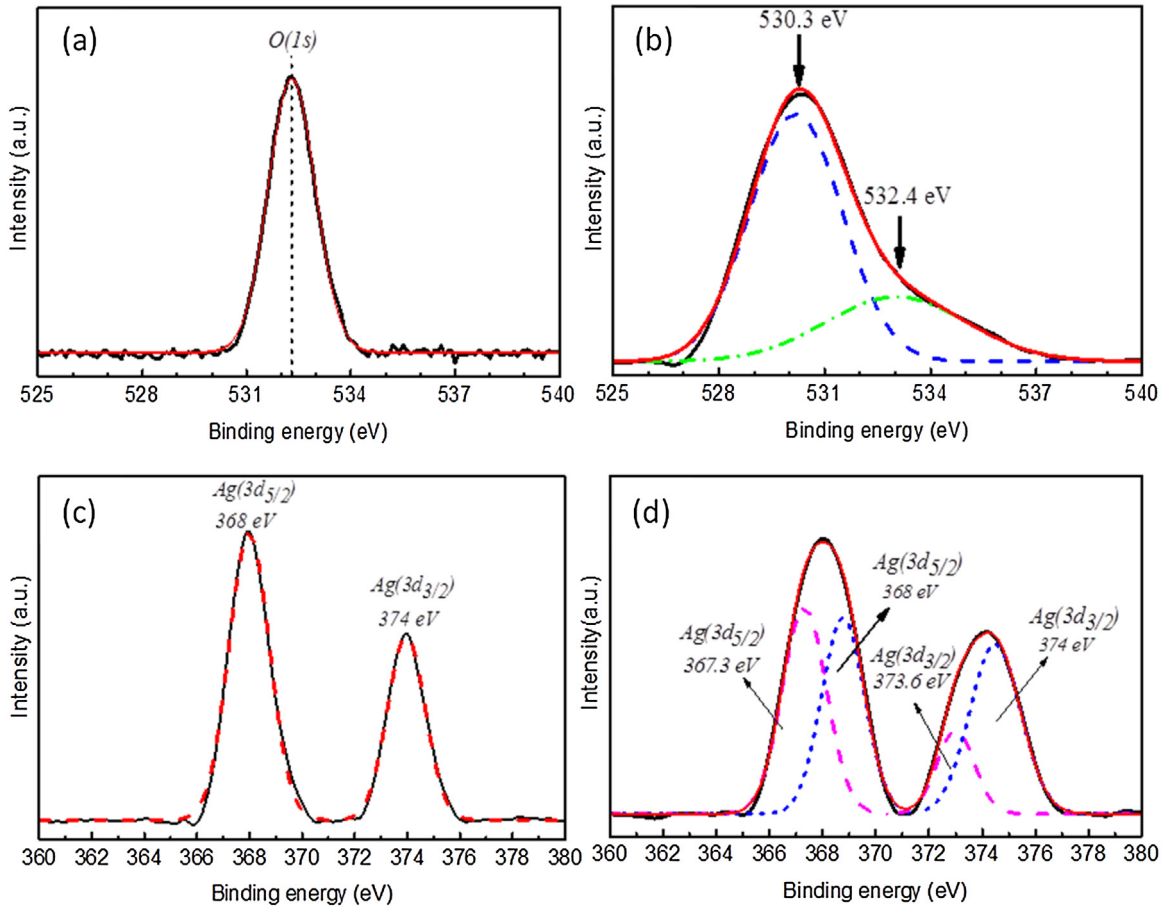

Fig. 3. High resolution XPS spectrum of the O1s feature for films grown using the TBH based process at a) 115 °C and b) 80 °C. The solid lines indicate the original XPS data and the dashed curves indicate theoretically fitted curves by assuming Gaussian distribution. High resolution XPS spectrum of the Ag3d peaks for films grown using the TBH based process at c) 115 °C and d) 80 °C. The solid lines indicate the original XPS data and the dashed curves indicate theoretically fitted curves by assuming Gaussian distribution.

which is consistent with oxygen in surface absorbates such as H_2O, O_2, CO_2 and CO [28]. The O1s feature for the film grown at 80 °C (Fig. 3b) is, however, more complex and is clearly made up of at least two peaks. A reasonable fit is obtained using two Gaussians centred at 530.3 eV and 532.4 eV, where the latter is once again attributed to surface absorbates. The peak at 530.3 eV suggests that some of the oxygen is bonded with the metal, which would be consistent with silver that is still associated with the hfac ligand.

For films growing in the ALD temperature window with TBH, two distinct Gaussian-like XPS peaks are observed at 368 eV ($Ag3d_{5/2}$) and 374 eV ($Ag3d_{3/2}$), which are attributed to Ag^0 species (Fig. 3c), consistent with the presence of metallic silver [29–31]. At growth temperatures below the ALD window (Fig. 3d), the $Ag3d_{5/2}$ peak becomes significantly broader and is best fitted with two Gaussians centred at 367.3 eV and 368 eV. The 367.3 eV peak is attributed to silver in the Ag-O bonding state [32,33] while the 368 eV peak is attributed to metallic silver. The XPS study shows that metallic silver is formed at all temperatures investigated, even down at 80 °C. While metallic silver is formed at temperatures below the window minima, the low thermal energy available results in incomplete reactions as already highlighted above. The un-reacted Ag(hfac)* species that remain on the surface at the end of one ALD cycle may act to block the chemisorptions of further Ag(hfac) species during the subsequent cycle, which could explain the observed decrease in growth rate at temperature below 105 °C.

3.3. Micro-structural study

The microstructure of the films grown at temperatures between 80 and 150 °C was studied using XRD (Fig. 4). Peaks at 38.2° and 44.4° are visible for all samples and are consistent with (111) and

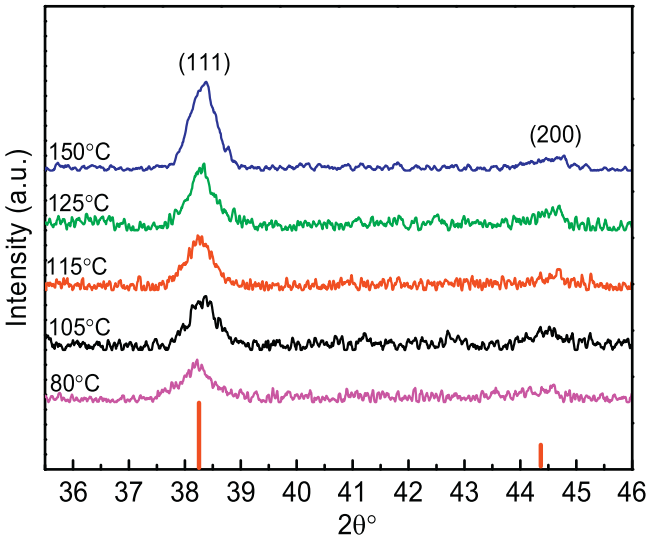

Fig. 4. X-ray diffraction patterns of silver coatings on Silicon (100) deposited at various temperatures using 0.2 s doses of TBH with 500 ALD cycles.

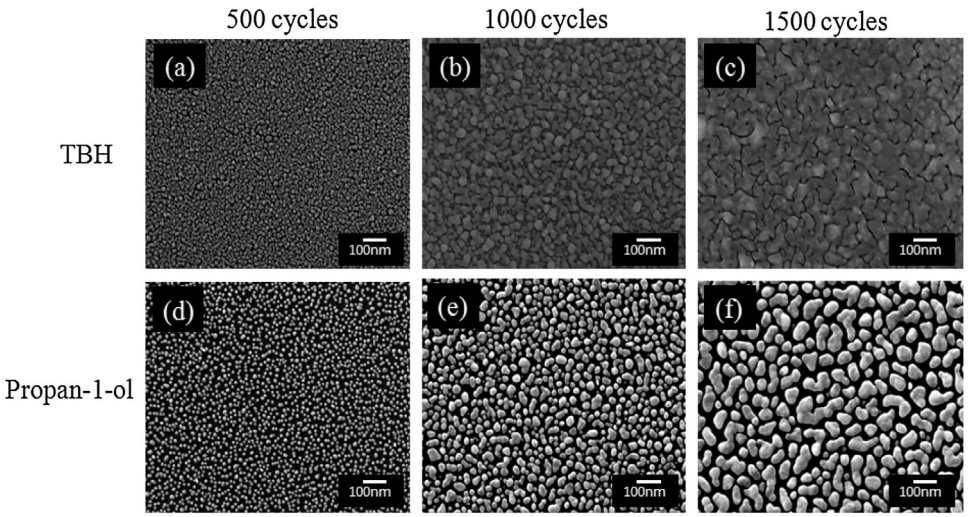

Fig. 5. SEM images of the surfaces at different number of ALD cycles on Si(100) with TBH for (a) 500 cycles [11 μg/cm^2], (b)1000 cycles [21 μg/cm^2] and (c) 1500 cycles [30 μg/cm^2], and with propan-1-ol for (d) 500 cycles [8 μg/cm^2], (e) 1000 cycle [13 μg/cm^2] and (f) 1500 cycles [19 μg/cm^2].

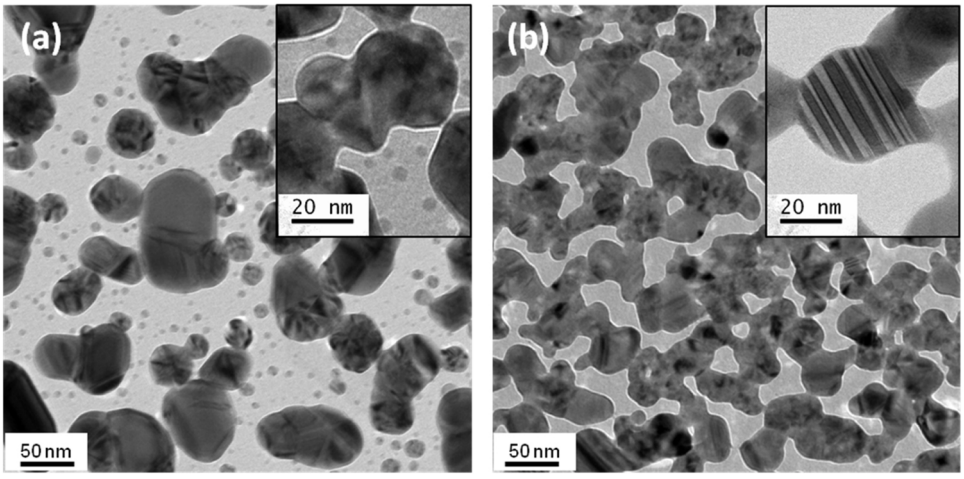

Fig. 6. High-resolution TEM images of ALD silver on SiN membranes for (a) propan-1-ol using 1000 cycles and (b) TBH using 750 cycles. Inset of figure (b)shows detail of twinning across an individual Ag island.

(200) reflection of face centred cubic (fcc) metallic silver (Fm-3m) (JCPDS 04-0783) respectively. Within the ALD window the XRD peak intensity and peak width remains almost constant indicating that the crystallite size and degree of crystalinity is independent of temperature within the ALD temperature range. The ratio between the peaks shows preferential orientation of the Ag grains along the (111) crystallographic direction [34]. As with the XPS, the XRD confirms the presence of crystalline metallic silver at 80 °C, which is well below the ALD window; for comparison, no XRD peaks were observed using propan-1-ol at 80 °C [11].

The choice of co-reactant is found to have a significant effect on the film morphology. Fig. 5 shows example SEM images of films grown using THB at 115 °C with 500 (Fig. 5a), 1000 (Fig. 5b) and 1500 (Fig. 5c) cycles and also using propan-1-ol at 125 °C with 500 (Fig. 5d), 1000 (Fig. 5e) and 1500 (Fig. 5f) cycles. Within the ALD window, temperature is found to have negligible effect on film morphology (see supplementary data), hence the differences in morphology are attributed to the co-reactant itself. As the growth rates of the two processes are different, it is perhaps best to compare films of comparable mass gains per unit area rather than cycle number. In this way, the best comparisons can be made between 500 cycles with TBH (Fig. 5a) and 1000 cycles with propan-1-ol (Fig. 5e), or between 1000 cycles with TBH (Fig. 5b) and 1500 cycles with propan-1-ol (Fig. 5f). As previously reported [11], the propan-1-ol based ALD process produces highly textured 'nano-particle' films in a Volmer-Weber [35] type growth mode (Fig. 5d–f). Silver films grown using TBH as a co-reactant (Fig. 5a–c) are also textured, however, the texturing appears significantly reduced compared to the propan-1-ol films. The TBH films appear to be almost planar, being made up of highly inner-connected platelets with narrow crevices. The growth with TBH is perhaps tending towards a Frank-van der Merwe growth mode [36]. After 1500 cycles the estimated coverage based on SEM image analysis is around 97% using TBH (compared to ~70% using propan-1-ol).

The difference in film morphology achieved using different co-reactants suggests some change in the interaction between the substrate surface and the growing films. A more detailed microstructural study was made to compare the morphology of the silver using propan-1-ol and TBH as shown in TEM micrographs in Fig. 6. In each case, the silver was deposited on SiN membranes at temperatures within the respective ALD windows for TBH and for the alcohol. The influence of the co-reagent on the growth habit, changes from a more three dimensional particulate morphology using the alcohol, to one that has a more two-dimensional platelet

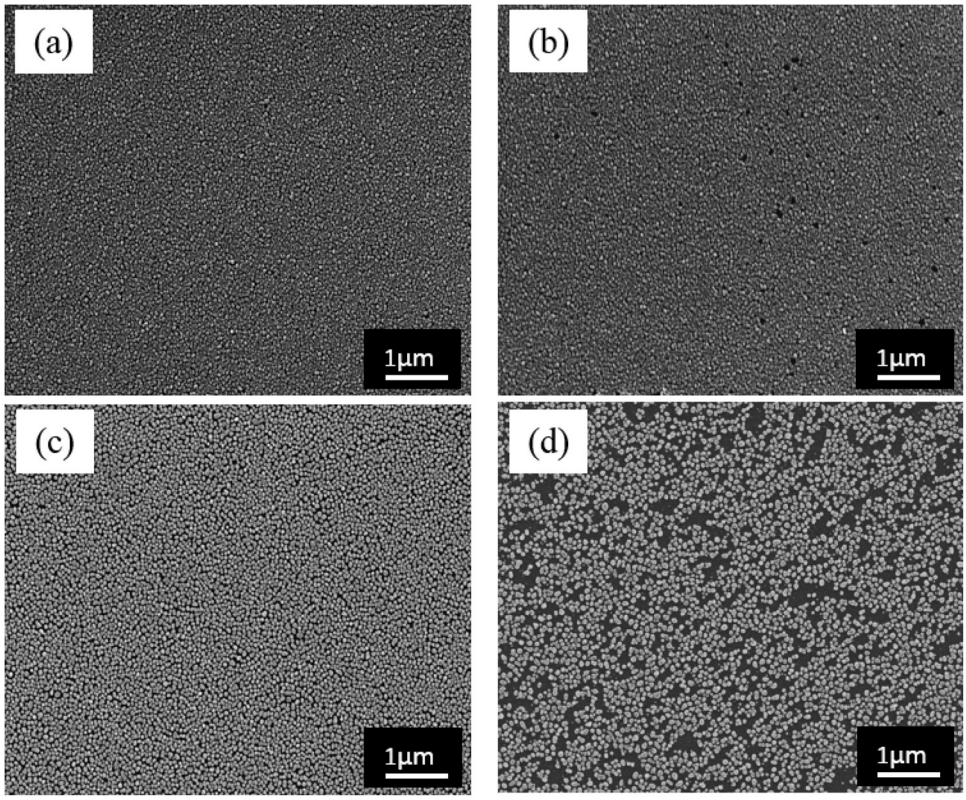

Fig. 7. Adhesion tape test results – SEM images of films deposited on Si(100) with either TBH or propan-1-ol before and after the tape test: (a) TBH before, (b) TBH after, (c) propan-1-ol before and (d) propan-1-ol after.

or island-like microstructure using the TBH. The difference in morphologies is attributed to the quite different Ag catalysed reaction for the alcohol, versus the direct surface reaction due to the decomposition of the TBH. The latter enhances surface diffusion so that growth can occur at the edges of the Ag islands, whereas the Ag catalysed propan-1-ol reaction promotes growth at the surface of the silver particles.

The influence of the TBH reaction with the substrate was investigated further using adhesion tests to evaluate the substrate-film bonding. Films with a nominal thickness of ~12 nm were assessed using SEM image analysis before and after the tape test (Fig. 7). Films deposited using TBH sustain an average aerial loss of around 5%, while films deposited using propan-1-ol show significantly more damage with a loss of around 40%. While the adhesion strength was not quantitatively evaluate, it is clear that the adhesion of silver is significantly higher for films grown using TBH than propan-1-ol. As the TBH is a powerful reducing agent, it is likely that it has an effect on the substrate surface during the early deposition cycles. We suspect that the TBH helps to remove atmospheric absorbents and other contaminants on the substrate surface akin to the 'self-cleaning' observed with trimethylaluminium (TMA) [37]. The 'cleaned' surface then promotes enhanced wetting and bonding of the silver on the surface, hence producing film like growth and improved adhesion.

3.4. Electrical properties

The electrical resistivity of films deposited on glass were investigated using four point probe measurements. Films grown using TBH at 115 °C were found to be conductive with resistivity decreasing from 0.62 Ω cm after 500 cycles (~9 nm), to 3×10^{-4} Ω cm after 1000 cycles (~18 nm) and 1×10^{-5} Ω cm after 1500 cycles (~27 nm). These values are slightly higher than best values reported for silver films grown using PE-ALD, where the lowest value of 6×10^{-6} Ω cm for 20 nm thick film has been reported [5,6]. All of the films grown using propan-1-ol were found to be insulating, even after 2000 cycles. This is attributed to the lack of interconnectivity between silver nanoparticles and, for films grown at temperatures below the ALD window, to non-metallic phases within the material.

3.5. Discussion on silver ALD using TBH

As highlighted by the results above, replacing propan-1-ol with TBH in the thermal ALD process for silver has a significant effect on both the process and the resulting films. We have previously shown that the alcohol based process relies on a catalytic conversion of the alcohol to the aldehyde and the reduction of the silver adsorbate to Ag^0 [11,13]. While this process permits self-limiting ALD, the reaction kinetics and thermal instability of the silver precursor are not well matched, resulting in a very narrow ALD temperature window. TBH has a much lower pKa value compared to alcohols such as propan-1-ol, hence TBH reacts more favourably. The enhanced reactivity of TBH compared either mono- or dimethyl hydrazine is explained by its ability to undergo an intra-molecular rearrangement (reaction 1), similar to a β-hydride elimination [21], in which the strong C—N bond can be broken more readily.

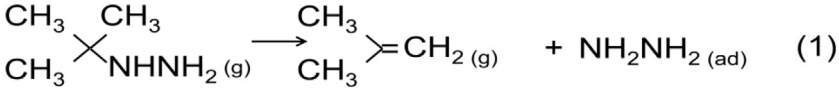

This phenomenon has been used previously to explain why when TBH is used in GaN growth, less carbon is incorporated in the growing film compared to using dimethyl hydrazine as a nitrogen source [21]. In the present study, the enhanced reactivity of the TBH with the silver precursor provides an explanation for the lower deposition temperatures achievable, compared with the alcohol-based ALD process. Furthermore the different growth habits observed using the alcohol (3D) and hydrazine (2D) is readily explained. The latter involves a surface mediated reaction between the silver adsorbate species and the hydrazine [38], in contrast to the catalytic step necessary when using the alcohol co-reagent. Accordingly the TBH can react directly at the substrate to generate the hydrogen required to decompose the Ag precursor. This assertion may also explain the better adhesion of the Ag films grown with TBH compared with the alcohol, as it is directly reactive with the growth surface, thereby influencing the bonding between the substrate and the silver overlayer.

4. Conclusions

For the first time, metallic silver has been deposited using self-limiting thermal ALD with a hydrazine-based co-reactant. The TBH co-reactant provides an ALD window between 105 and 128 °C, offering a 23 °C wide temperature range in which the growth is controlled by self-limiting surface reactions. The relatively wide ALD window achieved using TBH (23 °C) is potentially very advantageous compared to the narrow ALD window obtained with the alcohol based process (5 °C) in terms of manufacturing. The wider temperature window makes thermal control less critical, which is especially useful for the coating of large, non-planar structures. The process is much more on-par with plasma or radical enhanced ALD for the production of silver films in terms of the ALD window width. Unlike the plasma or radical enhanced ALD processes, the TBH process does not use co-reactant species that are lifetime-limited; hence the process is potentially advantageous for coating three dimensional high-aspect ratio structures. Within the ALD temperature window, the surface reactions produce crystalline metallic silver layers that are film-like, conductive and with no measureable fluorine contamination.

Acknowledgements

The authors would like to thank the Engineering and Physical Sciences Research Council (EPSRC) Knowledge Transfer Account (EP/H500146/1) for part funding this research. We also gratefully acknowledge the fruitful discussions with Paul Williams (Pegasus Chemicals Ltd) regarding the use of hydrazine coreagents in this study. All data created during this research is openly available from the University of Liverpool data catalogue at: http://datacat.liverpool.ac.uk.

Appendix A. Supplementary data

Supplementary data associated with this article can be found, in the online version, at http://dx.doi.org/10.1016/j.apsusc.2016.11.192.

References

[1] Q.H. Tran, V.Q. Nguyen, A.T. Le, Silver nanoparticles: synthesis, properties, toxicology, application and perspectives, Adv. Nat. Sci.: Nanosci. Nanotechnol. 4 (2013) 033001.
[2] R. Gupta, M.J. Dyer, W.A. Weimer, Preparation and characterization of surface plasmon resonance tunable gold and silver films, J. Appl. Phys. 92 (2002) 5264.
[3] J.V. Wittemann, W. Münchgesang, S. Senz, V. Schmidt, Silver catalyzed ultrathin silicon nanowires grown by low-temperature chemical-vapor-deposition, J. Appl. Phys. 107 (2010) 096105.
[4] S. Guo, E. Wang, Noble metal nanomaterials: controllable synthesis and application in fuel cells and analytical sensors, Nano Today 6 (2011) 240–264.
[5] A. Niskanen, T. Hatanpää, K. Arstila, M. Leskelä, M. Ritala, Radicaläenhanced atomic layer deposition of silver thin films using phosphineäadducted silver carboxylates, Chem.Vap. Deposition 13 (2007) 408–413.
[6] M. Kariniemi, J. Niinistö, T. Hatanpää, T. Kemell, M. Sajavaara, M. Leskelä, Plasma-enhanced atomic layer deposition of silver thin films, Chem. Mater. 23 (2011) 2901–2907.
[7] F.J. Van den Bruele, M. Smets, A. Illiberi, Y. Creyghton, P. Buskens, F. Roozeboom, P. Poodt, Atmospheric pressure plasma enhanced spatial ALD of silver, Vac. Sci. Technol. A 33 (2015) 01A131.
[8] A.A. Amusan, B. Kalkofen, H. Gargouri, K. Wandel, C. Pinnow, M. Lisker, E.P. Burte, Ag films grown by remote plasma enhanced atomic layer deposition on different substrates, J. Vac. Sci. Technol. A 34 (2016) 01A126.
[9] S.S. Masango, L. Peng, L.D. Marks, R.P. Van Duyne, P.C. Stair, Nucleation and growth of silver nanoparticles by AB and ABC-type atomic layer deposition, J. Phys. Chem. C 118 (2014) 17655–17661.
[10] P.R. Chalker, S. Romani, P.A. Marshall, M.J. Rosseinsky, S. Rushworth, P.A. Williams, Liquid injection atomic layer deposition of silver nanoparticles, Nanotechnology 21 (2010) 405602.
[11] Z. Golrokhi, S. Chalker, C.J. Sutcliffe, R.J. Potter, Self-limiting atomic layer deposition of conformal nanostructured silver films, Appl. Surf. Sci. 364 (2016) 789–797.
[12] H.B. Profijt, S.E. Potts, M.C.M. Van de Sanden, W.M.M. Kessels, Plasma-assisted atomic layer deposition: Basics, opportunities, and challenges, J. Vac. Sci. Technol. A 29 (2011) 050801.
[13] P.A. Bahlawane, Premkumar, G. Brechling, K. Kohse-Hoeinghaus, Alcohol-Assisted CVD of silver using commercially available precursors, Chem. Vap. Deposition 13 (2007) 401–407.
[14] B. Zhao, T. Momose, T. Ohkubo, Y. Shimogaki, Acetone-assisted deposition of silver films in supercritical carbon dioxide, Microelectron. Eng. 85 (2008) 675–681.
[15] S. Rushworth, P. Williams (2011), U.S. Patent Application No. 13/635, 478.
[16] B.B. Burton, A.R. Lavoie, S.M. George, Tantalum nitride atomic layer deposition using (tert-Butylimido) tris (diethylamido) tantalum and hydrazine, J. Electrochem. Soc. 155 (2008) D508–D516.
[17] Z. Fang, H.C. Aspinall, R. Odedra, R.J. Potter, Atomic layer deposition of TaN and Ta 3N 5 using pentakis (dimethylamino) tantalum and either ammonia or monomethylhydrazine, J. Cryst. Growth 331 (2011) 33–39.
[18] M. Juppo, M. Ritala, M. Leskelä, Use of 1, 1-Dimethylhydrazine in the atomic layer deposition of transition metal nitride thin films, J. Electrochem. Soc. 147 (2000) 3377–3381.
[19] T.J. Knisley, T.C. Ariyasena, T. Sajavaara, M.J. Saly, C.H. Winter, Low temperature growth of high purity, low resistivity copper films by atomic layer deposition, Chem. Mater. 23 (2011) 4417–4419.
[20] G. Dey, S.D. Elliott, Copper reduction and atomic layer deposition by oxidative decomposition of formate by hydrazine, RSC Adv. 4 (2014) 34448–34453.
[21] Y.J. Hsu, L.S. Hong, J.E. Tsay, Metalorganic vapor-phase epitaxy of GaN from trimethylgallium and tertiarybutylhydrazine, J. Cryst. Growth 252 (2003) 144–151.
[22] S. Acharya, G. Neogi, R.K. Panda, D. Ramaswamy, Kinetics of oxidation of hydrazine and of t-butylhydrazine using tris (dimethylglyoximato) nickelate (IV) in the presence of added Cu^{2+}(aq), J. Chem. Soc. Dalton Trans. (1984) 1477–1484.
[23] National Center for Biotechnology Information, PubChem Compound Database; CID = 1031, 2016, https://pubchem.ncbi.nlm.nih.gov/compound/1031 (Accessed September 2016).
[24] S. Hindley (2014). Atomic layer deposition and metal organic chemical vapour deposition of materials for photovoltaic applications (Chapter 5 of Doctoral dissertation, University of Liverpool).
[25] R.J. Potter, P.R. Chalker, T.D. Manning, H.C. Aspinall, Y.F. Loo, A.C. Jones, L.M. Smith, G.W. Critchlow, M. Schumacher, Deposition of HfO_2, Gd_2O_3 and PrO_x by liquid injection ALD techniques, Chem. Vap. Dep. 11 (2005) 159–169.
[26] C.A. Schneider, W.S. Rasband, K.W. Eliceiri, NIH Image to ImageJ: 25 years of image analysis, Nat. Methods 9 (2012) 671–675.
[27] D.M. Bastidas, E. Cano, A.G. Gonzalez, S. Fajardo, R. Lleras-Pérez, E. Campo-Montero, J.M. Bastidas, An XPS study of tarnishing of a gold mask from a pre-Columbian culture, Corros. Sci. 50 (2008) 1785–1788.
[28] Z. Shi, J. Zhang, D. Gao, Z. Zhu, Z. Yang, Z. Zhang, D. Xue, Magnetic resonance of the NiFe2O4 nanoparticles in the gigahertz range, Nanoscale Res. Lett. 8 (2013) 1–5.
[29] J. Guo, H. Wu, X. Liao, B. Shi, Facile synthesis of size-controlled silver nanoparticles using plant tannin grafted collagen fiber as reductant and stabilizer for microwave absorption application in the whole Ku band, J. Phys. Chem. C 115 (2011) 23688–23694.
[30] A. Yang, G. Wolcott, A. Wang, R.C. Sobo, F. Fitzmorris, J.Z. Qian, Zhang, Y. Li, Nitrogen-doped ZnO nanowire arrays for photoelectrochemical water splitting, Nano Lett. 9 (2009) 2331–2336.
[31] S. Thomas, S.K. Nair, E.M.A. Jamal, S.H. Al-Harthi, M.R. Varma, M.R. Anantharaman, Size-dependent surface plasmon resonance in silver silica nanocomposites, Nanotechnology 19 (2008) 075710.
[32] S. Ferraris, M. Ferraris, S. Miola, C. Perero, E. Vernè, G. Gautier, A. Manfredotti, E. Battiato, G. Speranza, I. Bogdanovic, Effect of thermal treatments on sputtered silver nanocluster/silica composite coatings on soda-lime glasses: ionic exchange and antibacterial activity, J. Nanopart. Res. 14 (2012) 1–19.

[33] P. Kumar, M.C. Mathpal, A.K. Tripathi, J. Prakash, A. Agarwal, M.M. Ahmad, H.C. Swart, Plasmonic resonance of Ag nanoclusters diffused in soda-lime glasses, Phys. Chem. Chem. Phys. 17 (2015) 8596–8603.
[34] R. Sun, H.Hou Hong, Z. Fan, J. Shao, Thickness dependence of structure and optical properties of silver films deposited by magnetron sputtering, Thin Solid Films 515 (2007) 6962–6966.
[35] L.K. Othaman, S. Boo, The Stranski?Krastanov three dimensional island growth predication on finite size model (Part I), J. Fiz. UTM 3 (2008) 78–83.
[36] D. Mishra, D. Greving, G.B. Confalonieri, J. Perlich, B.P. Toperverg, H. Zabel, O. Petracic, Growth modes of nanoparticle superlattice thin films, Nanotechnology 25 (2014) 205602.
[37] W. Jevasuwan, Y. Urabe, T. Maeda, N. Miyata, T. Yasuda, H. Yamada, M. Hata, N. Taoka, M. Takenaka, S. Takagi, Initial processes of atomic layer deposition of Al_2O_3 on InGaAs: interface formation mechanisms and impact on metal-insulator-semiconductor device performance, Materials 5 (2012) 404–414.
[38] D. Cheng, S. Xia, J. Tong, The mechanism of directional oxidation of hydrazine by silver coordination compounds, Transit. Met. Chem. 21 (1996) 503–506.